Current Biology 19, 335–340, February 24, 2009 ©2009 Elsevier Ltd All rights reserved DOI 10.1016/j.cub.2009.01.041

Report

Characterization and Coding of Behaviorally Significant Odor Mixtures

Jeffrey A. Riffell,[1,*] Hong Lei,[1] Thomas A. Christensen,[1,2] and John G. Hildebrand[1]
[1]Arizona Research Laboratories Division of Neurobiology
[2]Department of Speech, Language & Hearing Sciences
University of Arizona
Tucson AZ 85721
USA

Summary

For animals to execute odor-driven behaviors, the olfactory system must process complex odor signals and maintain stimulus identity in the face of constantly changing odor intensities [1–5]. Surprisingly, how the olfactory system maintains identity of complex odors is unclear [6–10]. We took advantage of the plant-pollinator relationship between the Sacred *Datura* (*Datura wrightii*) and the moth *Manduca sexta* [11, 12] to determine how olfactory networks in this insect's brain represent odor mixtures. We combined gas chromatography and neural-ensemble recording in the moth's antennal lobe to examine population codes for the floral mixture and its fractionated components. Although the floral scent of *D. wrightii* comprises at least 60 compounds, only nine of those elicited robust neural responses. Behavioral experiments confirmed that these nine odorants mediate flower-foraging behaviors, but only as a mixture. Moreover, the mixture evoked equivalent foraging behaviors over a 1000-fold range in dilution, suggesting a singular percept across this concentration range. Furthermore, neural-ensemble recordings in the moth's antennal lobe revealed that reliable encoding of the floral mixture is organized through synchronized activity distributed across a population of glomerular coding units, and this timing mechanism may bind the features of a complex stimulus into a coherent odor percept.

Results

In the Southwestern USA the bouquet from *Datura wrightii* flowers evokes innate foraging behavior in *Manduca sexta* moths [11, 12], and this odor is therefore an excellent tool for examining the neural basis by which complex odors are processed in the antennal (olfactory) lobe (AL) of the moth's brain. As a first step in investigating how AL neurons encode complex mixture stimuli, we used gas chromatography with mass-spectrometric detection (GCMS) and tandem gas chromatography-multi-channel recording (GCMR) [13, 14] to determine the behaviorally critical odorants from the *D. wrightii* floral bouquet. GCMS analysis of the *D. wrightii* floral scent revealed more than 60 compounds that varied in identity and concentration (Table S1 and Figure S1 in the Supplemental Data available online). In contrast to the complexity of the floral scent, GCMR recordings (Figure 1A) of the neural-ensemble responses to the gas chromatography (GC) eluates revealed that neurons responded to only a fraction (15%) of those components. Data from this system revealed specific patterns of odorant-evoked activity across multiple units (Figure 1B). As an independent factor, the concentration per se of all the eluted odorants (0.1–450 ng/μl) had no influence on the activity of any single unit or the ensemble (Figures S2A and S2B; mixed effects, repeated-measures (rm) regression for single units: $p = 0.65$; rm regression for ensemble: $p = 0.81$). Rather, the neural response resided in the selectivity for certain odorants.

An analysis of population-level responses demonstrated strong ensemble selectivity for a group of nine odorants (Figure 1C). To examine odorant-evoked responses between preparations ($n = 16$), we calculated the percentage of excited units (response index [RI] ≥ 2.0) in each ensemble for each odorant (Figure 1D). This analysis confirmed that many units were activated by one or more members of this same group of nine odorants: benzaldehyde (*bea*), benzyl alcohol (*bol*), linalool (*lin*), nerol (*ner*), β-myrcene (*myr*), methyl salicylate (*mal*), geraniol (*ger*), *E*-caryophyllene (*car*), and α-farnesene (*far*) (odorants 23–31, respectively). The remaining odorants evoked little or no activity in most units. There were significant differences between odorants in their activation potency (rm ANOVA: $p < 0.0001$): the nine odorants activated significantly higher percentages of units than the majority (47/51) of the other floral compounds (Figure 1E; post-hoc Fisher's test: $p < 0.01$). Testing the synthetic homologs of these nine headspace odorants revealed similar unit and ensemble responses (Figures S3A–S3C). Thus, the ensemble analysis of unit responses revealed a strong preference for only a small subset of compounds emitted by *D. wrightii* flowers.

Behavioral Responses: Mixture at Different Concentrations versus Single Odorants

A critical question is: are the potent odorants that we have identified through GCMR analysis, either singly or as a mixture, behaviorally effective? To examine the behavioral saliency of these stimuli, wind-tunnel experiments were conducted.

A striking finding was that moths were not attracted by the single odorants. Behavioral measurements evoked by single odorants were not statistically different from those evoked by controls (mineral oil, no odor) (Figure 2A; Table S3; *G* test: $p > 0.25$), and the moths exhibited random flight trajectories typical of search behaviors (Figure 2A, top) [15, 16]. Only the single odorants *bea* and *bol* elicited feeding responses (Figure 2A), but those responses, and the responses to the two-component mixture of those odorants, were not significantly different from those elicited by the control (Table S3). In contrast, both the mixture of the nine key synthetic compounds and the natural scent from *D. wrightii* flowers evoked robust behavioral responses in which moths fed from flowers significantly more often than in the single-odorant and control conditions (Figure 2A; *G* test: $p < 0.0001$). Moreover, behavioral responses to the synthetic odor mixture and the *D. wrightii* scent were not significantly different from one another (*G* test all behaviors: $p > 0.25$). Thus, the

*Correspondence: jeffr@neurobio.arizona.edu

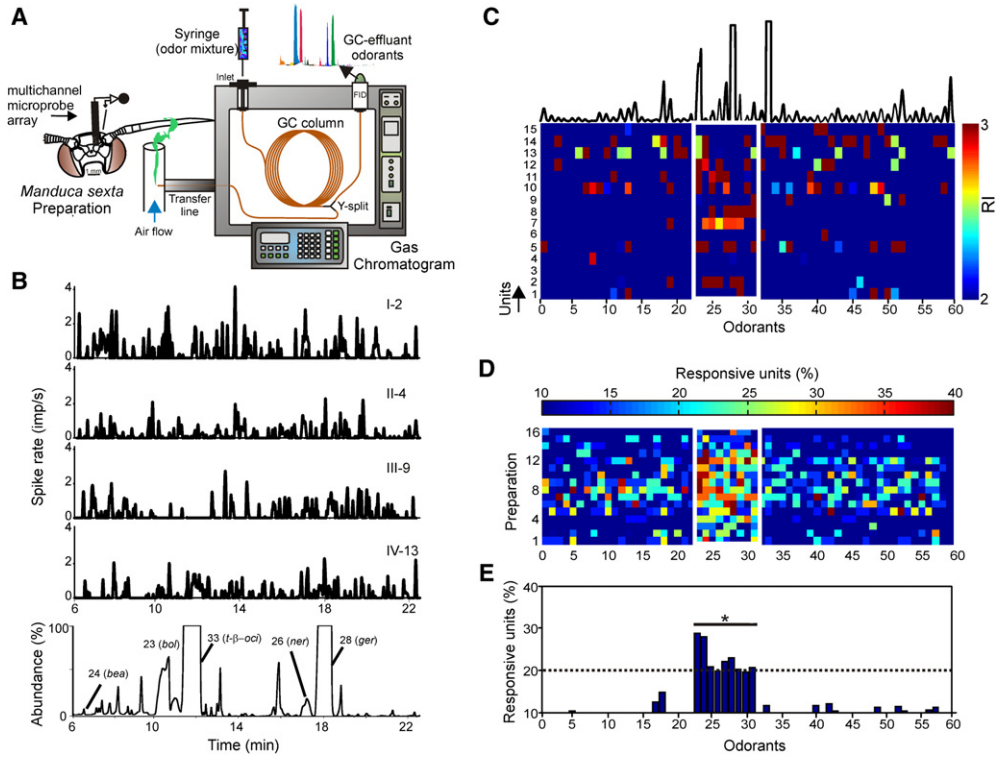

Figure 1. Multiunit Responses to GC-Fractionated Odor from the *D. wrightii* Flower

(A) Schematic representation of a combined GCMR experiment. The floral odor was trapped through dynamic headspace sorption and eluted with a solvent (hexane). The floral extract was injected in the heated injection port of the gas chromatograph, thereby volatilizing the sample. The effluent from the column was split such that half of the flow enters the gas chromatograph's flame-ionization detector, which ionizes compounds and produces a voltage signal. The other half of the effluent was carried by a heated transfer line and arrived simultaneously at the moth's antenna. Action potentials from the AL neural ensemble were continuously recorded extracellularly during the 20 min of odor delivery via GC.

(B) Rate histograms (bin size, 100 ms) of unit responses to the eluting compounds from the *D. wrightii* headspace extract (1 μl injection) (bottom trace). Each unit was recorded from one of the four shanks on the electrode recording array, with the Roman numeral denoting the shank number, and number corresponding to the unit on that shank. Certain odorants (e.g., benzyl alcohol (*bol*, odorant 24) and nerol (*ner*, odorant 26) evoked significant responses in units on different shanks.

(C) Ensemble representations for each odorant eluted from the gas chromatograph. The top plot shows the chromatogram with each peak corresponding to an odorant (numbered on the *x* axis). Odorants 28 and 33 (geraniol and *trans*-β-ocimene, respectively) constituted 81% of the total odorant concentration. Only the excitatory responses with a response index (RI) $\geq$ 2.0 SDs are shown for clarity (color scale). Note that the ensemble responses clustered around a small group of nine odorants (23–31; outlined by a white box) within the floral headspace. Odorant number corresponds to the retention time, except for those odorants that gave robust responses (odorants 23–31), which were rearranged for clarity.

(D) The percentage of responsive units in each ensemble (threshold RI $\geq$ 2.0) was determined for each odorant in the floral headspace and plotted for each preparation (n = 16). Ensemble responses to odorants 23–31 are framed by a white box for clarity.

(E) A threshold of 2 standard deviations (dotted line) of the entire data set was used to identify the odorants that evoked the greatest activity: benzaldehyde (*bea*), benzyl alcohol (*bol*), linalool (*lin*), nerol (*ner*), β-myrcene (*myr*), methyl salicylate (*mal*), geraniol (*ger*), caryophyllene (*car*), and α-farnesene (*far*). The asterisk denotes a significant difference (multiple comparisons: $p < 0.05$) between odorants 23–31 and a majority of the remaining odorants (47/51).

nine-component synthetic mixture appears to be an excellent mimic of the natural floral odor.

A key question, however, is whether other odorants and mixtures that are from the *D. wrightii* bouquet but that are not identified by the GCMR technique as potent odorants could elicit similar behavior. We conducted two experimental tests to answer this question. The first experiment tested a random mixture of nine odorants from the *D. wrightii* flower (Table S2). Moth foraging responses were significantly reduced with the random mixture as compared to the natural *D. wrightii* scent or the mimic (Figure 2A) (*G* test: $p < 0.001$). In the second experiment, two-choice tests were conducted in which moths were simultaneously exposed to the *D. wrightii* flower and the *D. wrightii* mimic. Moths exposed to the two flowers fed from both at equal frequencies (Figures S4A and S4B; *G* test: $p > 0.50$), thus demonstrating the behavioral significance of the mixture revealed by GCMR.

Moths also responded similarly to the *D. wrightii* odor mimic over a wide range of concentrations. To evaluate the dose-response relationship for the *D. wrightii* odor mimic, we tested the synthetic mixture at dilutions of 1.0 to 0.001 in the wind tunnel. Even when the mixture was diluted 1000-fold—and hence was presented at a concentration less than or nearly equal to that of any of the single odorants in the natural mixture—behavioral responses were not statistically different from responses to the highest mixture concentration (one-way ANOVA for mixture concentration: $p = 0.92$; post-hoc Fisher's test: $p > 0.30$). Moreover, all mixture concentrations produced significantly greater behavioral responses than the single odorants, the two-component mixture of *bea* and *bol*, or the control (Figures 2A and 2B;Table S3; Figure S5), suggesting consistent perception of this odor mixture over a 1000-fold range in concentration.

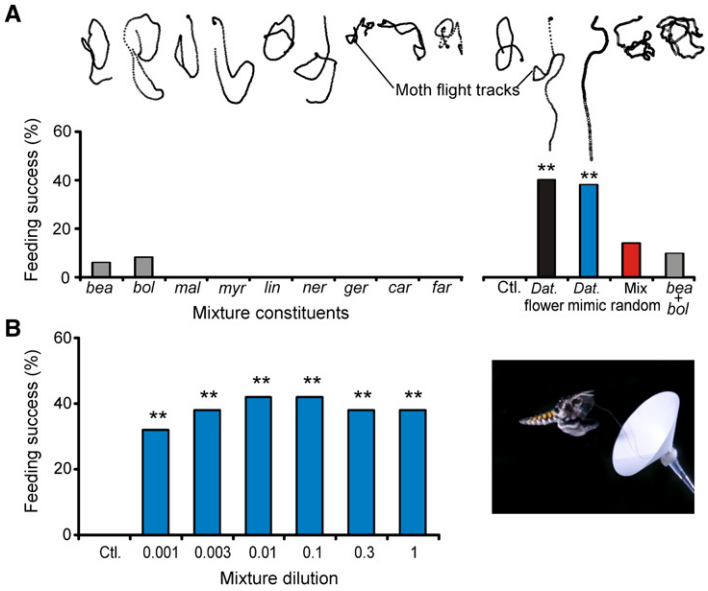

Figure 2. Odor-Modulated Flight Behavior as a Response to Mixtures

(A) Top: Moths' flight tracks to the mixtures (synthetic mixture containing nine components, two-component mixture of *bea* and *bol*, and the natural floral odor) and the single odorants. Note the straight trajectories of the moth flight track to the nine-component mixture and *D. wrightii* scent. Each circle corresponds to a time point of 16.6 ms. Bottom: Percentage of moths feeding from the odor source. n = 20–50 moths per odor stimulus treatment.

(B) Left: The effects of mixture concentration on feeding behavior of moths. Mixtures 0.001–1 yielded results not significantly different from one another (post-hoc Fisher's test: $p > 0.22$). Asterisks denote a significant difference from the (negative) mineral-oil control (*G* test: $^{**}p < 0.01$). Right: Image of a naive male moth feeding from a paper flower loaded with the nine-component odor mixture (image courtesy of C. Hedgcock).

Unit Responses: Characteristics of Mixtures and Single Odorants

How is the behaviorally relevant floral mixture encoded in the AL, and is there a mechanism by which the mixture is efficiently encoded even as stimulus concentration changes? To address these questions, we first examined mixture interactions at the single-unit level. Using the terminology of [17] to classify mixture interactions based on psychophysical studies, we characterized unit responses as (i) suppression, (ii) hypoadditivity, and (iii) synergy on the basis of each unit's response to the mixture relative to the response to the most effective component (Figures 3A–3C). Among the units responsive (excited or inhibited) to the tested odors (60%), there were significant differences between response classes (ANOVA: $p < 0.0001$); most units (42%) exhibited hypoadditive responses to the mixture, and fewer exhibited suppression (11%) or synergy (7%) (post-hoc Fisher's test: $p < 0.0001$). The synergistic or suppression-elicited responses to these units, however, did not occur at a 10-fold decrease in mixture concentration (Figures 3B and 3C).

Behavioral responses might be due to a higher number of activated units in response to the mixture, or they could be due to those units that showed synergistic responses. We therefore examined unit responses as a function of mixture concentration. First, no units (0/8 units) exhibited synergistic responses to the lower mixture concentrations (0.01–0.001) (Figure 3D; Kuskal-Wallis test with multiple comparisons: $p > 0.05$). Second, for all the responsive units, stimulus type (mixture versus odorant) had a significant effect on the percentage of responsive units (Kuskal-Wallis test: $p < 0.01$); the synthetic mixture and floral extract yielded significantly higher values than the single odorants (Figure 3E; Kuskal-Wallis test with multiple comparisons: $p < 0.05$). When the mixture concentration was decreased, however, differences in the percentage of responsive units and also response type (e.g., activation and inhibition) between mixtures and single odorants became nonsignificant (Figure 3E; $p > 0.05$). Thus, neither the units that exhibit synergy to the mixture nor the percentage of responsive units alone can explain the behavioral consistency across this concentration range (Figure 2). The neural code underlying the observed singular perception of odor mixtures must reside in other domains of the odor-evoked glomerular representations.

Spatiotemporal Coordination of Ensemble Responses to Mixtures and Single Odorants

We next investigated the spatial distribution and temporal relationships of units in response to mixtures or single odorants by using a spatially defined 16-channel tetrode recording array. As a first step toward understanding how the mixtures are encoded, we examined the spatial distribution of ensemble responses. Prior to stimulation, units were spontaneously active (Figure 4A, top), but upon odor stimulation ensemble activity significantly increased (RI $\geq$ 2.0), and there was an overlap in unit responses between the single odorant *ger* and the mixtures 10° and 10^{-1} (Figure 4A, bottom). To compare the ensemble representations between different odor stimuli, we used two different analyses. The first analysis was the correlation coefficient between ensemble responses to two different stimuli (see Supplemental Experimental Procedures, Equation S4) [7, 18]. The second analysis examined the relationship between odor-evoked responses of different stimuli in multivariate space through the normalized Euclidean distances between odors (dissimilarity index) (see Supplemental Experimental Procedures, Equation S5) [9, 19, 20]. These two different measures together provide the means to examine the relationships between odor-evoked responses. First, on the basis of the spatial distribution of activated units, the correlations between stimulus pairs revealed a broad degree of response overlap between mixtures (Figures 4B and 4C; Spearman's rank test: $r \geq 0.68$, $p < 0.05$), but the lowest-concentration mixture was also significantly correlated with many of the individual odorants, including *bol, ger, lin,* and *bea* (Spearman's rank test: $r \geq 0.53$, $p \leq 0.06$). In fact, for all preparations, the lower mixture concentrations were as correlated to the other mixtures as to the individual odorants (Figures S6A and S6B; Spearman's *r* for mixtures: $r = 0.36$, ± 0.09 SEM; Spearman's *r* for odorants: $r = 0.29$, ± 0.07 SEM; Mann-Whitney *U* test: $p = 0.59$). These results were similarly reflected in the dissimilarity indices between stimuli, where the lower mixture concentrations (0.1–0.001) were not statistically dissimilar to those of the single odorants (Figure 4D; Mann-Whitney *U* test: $p \geq 0.29$). These results suggest that the spatial distribution pattern of ensemble responses alone does not fully explain the behavioral efficacy of the mixtures relative to the single odorants or the behavioral consistency of the mixtures across concentrations.

We next examined how temporal relationships between units in the ensemble, through synchronous firing, might effectively encode the behavioral significance of the odor mixtures.

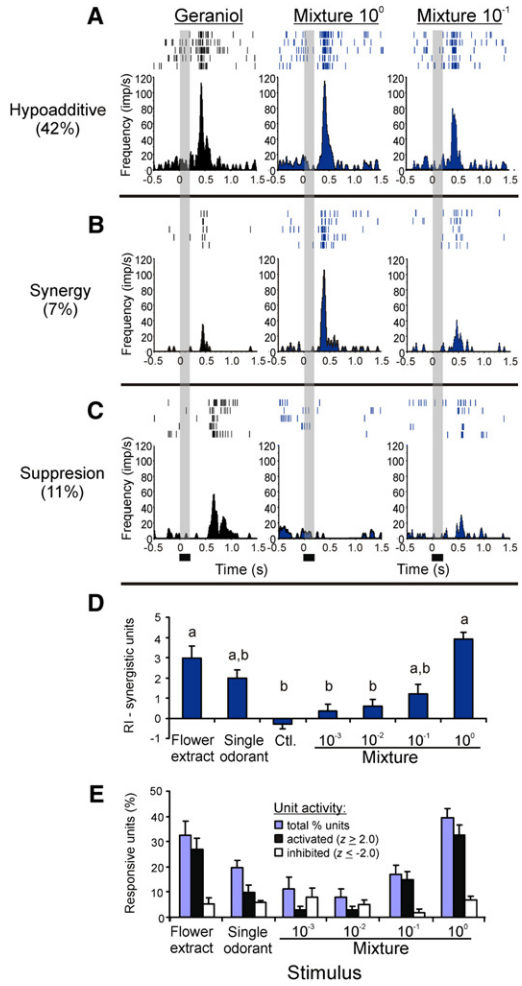

Figure 3. Unit Responses to Mixtures and Single Odorants

(A–C) Units that showed similar ("hypoadditive") (A), synergistic (B), or suppressive (C) responses to the mixture (middle and right-most columns) relative to the single odorants (left-most column) that evoked the greatest responses. For these three units (each from a different preparation), geraniol elicited the greatest response. Gray bars denote the stimulus duration (200 ms). There was a delay of 350 ms delay from the odor onset to the time the stimulus reached the preparation. Note that the suppression- and synergy-evoked responses changed with mixture concentration.

(D) The response indices (RIs) of those units that showed synergy to the initial mixture concentration. Values are the means ± SEM. Letters denote a significant difference ($p < 0.05$) between odor stimuli. (E) Percentage of units responsive to the individual odorants and mixtures. Unit responses were further repartitioned into the percentage of cells activated ($z \geq -2.0$) and inhibited ($z \leq 2.0$) by the odorants or mixtures. Values are the means ± SEM.

Recent evidence has demonstrated that odor identity can also be coded through the temporal relationships between AL (or olfactory bulb) neurons [9, 18, 21, 22], but it remains unclear whether the temporal features of the ensemble response can effectively code for mixtures. Similar to the RI activity by the units, prior to stimulation different subsets of units were spontaneously active, but none of them showed >10% synchronous activity (Figure 4A, top). Odor stimulation, on the other hand, greatly enhanced synchronous firing between pairs of units (see Supplemental Experimental Procedures) (Figure 4A, bottom; Figure S7). To quantify differences in synchrony patterns elicited by different olfactory stimuli (Figure 4E), we calculated correlation coefficients between all stimulus pairs. In the example shown in Figure 4F, the correlation between the floral extract and all mixtures was significantly greater (Spearman's rank test: $r \geq 0.21$, ± 0.03 SEM; $p < 0.05$) than that for the floral extract or single odorants (mean $r = 0.01$, ± 0.01 SEM; $p > 0.21$). We obtained similar results when we compared the mixtures among themselves versus the single odorants (white box in Figure 4F). Unlike the results in Figure 4C, which were based only on the spatial distribution of ensemble responses, the result of the synchrony correlation analysis across all mixture concentrations was fully consistent with our behavioral observations (Figure 2B). In addition, mixtures were significantly more correlated than the single odorants in all preparations (Figure S6C; Mann-Whitney *U* test: $p < 0.05$, n = 8 moths), again suggesting a qualitative difference between mixture-evoked (regardless of concentration) and single-odorant-evoked synchrony patterns. These results were further verified with the dissimilarity indices between odor stimuli, where the synchrony patterns evoked by the mixtures were statistically more similar to one another than to those evoked by the single odorants (Figure 4G; Mann-Whitney *U* test: $p \leq 0.01$). Synchrony patterns, therefore, provide a means by which behaviorally effective mixtures can be encoded by the olfactory system even with changing concentration.

Heterogeneity of Unit-Pair Contributions to the Pattern of Ensemble Synchrony

Our results suggest that ensemble synchrony might be a coding mechanism for mixture stimuli, but the manner in which the neural synchrony might encode the mixtures remains uncertain. For instance, the olfactory system might rely on the number of synchronous cell pairs (SI ≥ 10%), the total magnitude of synchrony in the ensemble, or the synchrony from a specific subset of neurons to represent the stimuli. We therefore examined each of these hypotheses in turn. We found that odor stimuli were not significantly different for either the percentage of synchronous cell pairs in the ensemble (Figure S8A; Kruskal-Wallis test: $p = 0.98$; multiple comparisons: $p > 0.05$) or the total magnitude of ensemble synchrony (Figure S8B; Kruskal-Wallis test: $p = 0.13$; multiple comparisons: $p > 0.05$). Thus, these potential coding mechanisms could not underlie the behavioral distinction between single odorants and odor mixtures. Next, to examine whether the synchrony of certain cell pairs might contribute more to coding the stimulus than others, we used a Procrustes analysis (PA) to compare ensemble responses between stimuli. The PA allows determination of those cell pairs that produce similar levels of synchrony in response to related stimuli (e.g., mixtures at different concentrations; see Supplemental Experimental Procedures for details). The PA revealed 10–20 cell pairs that produced similar levels of synchrony between mixtures (Figure S9A). Are these the cell pairs that encode the mixture stimuli, and how sensitive is this coding mechanism to the loss of the cell pairs contributing to the representation? A sensitivity analysis revealed that removal of those crucial cell pairs caused mixture representations to become dissimilar from one another; removal of only 10–20 cell pairs elicited this effect (arrow in Figure S9B). Moreover, removal of these crucial cell pairs caused all mixture concentrations to become significantly dissimilar from one another (Kruskal-Wallis test with multiple comparisons: $p < 0.05$), implying a fictive breakdown of behavioral consistency over these mixture intensities (Figure S9C). Removal of these critical cell

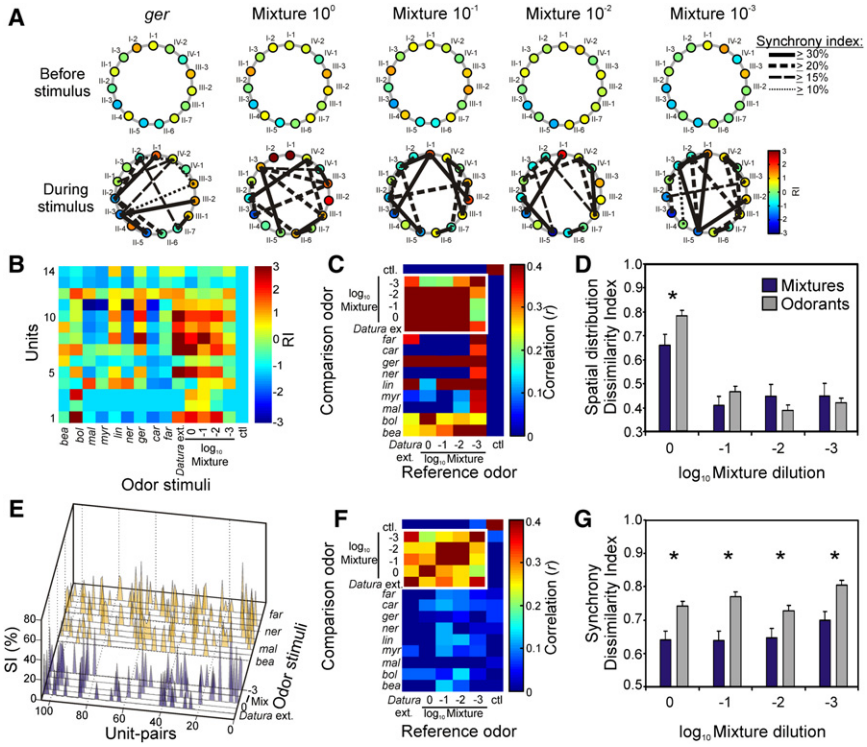

Figure 4. Spatiotemporal Processing of Odor Mixtures

(A) Spatial activity and synchrony between units. The spatial response pattern for the 15-unit ensemble is represented as a circular matrix in which individual units are ordered clockwise starting from the 12:00 position (unit I-1). Each unit is represented as a circle around the perimeter of the matrix, and its RI is represented by the circle color (see color scale). Also shown are the synchrony patterns (solid, dashed, and dotted lines connecting unit pairs) that underlie the ensemble response to each stimulus; each connecting line represents the synchrony (after shuffle correction) between specific unit pairs.

(B) The color-coded response matrix from a 14-unit ensemble (different preparation from [A] recorded after stimulation with the different odorants and mixtures (columns).

(C) Pair-wise correlations between mixtures (reference stimuli) and between single odorants and mixtures (comparison stimuli) on the basis of the spatial distribution of activated units in the ensemble shown in (B). Correlation coefficients between odor pairs are color coded.

(D) The dissimilarity indices of the mixtures to one another (blue bars) or to the single odorants (gray bars) on the basis of the spatial distribution of activated units (n = 8 preparations). Values are the means ± SEM.

(E) The synchrony coefficients (SI%) of unit pairs in response to behaviorally effective mixtures (blue) and single odorants (yellow). Note that both mixtures and single odorants elicited SI values > 30% in individual unit pairs.

(F) The pair-wise correlation of the ensemble synchrony patterns between different odor stimuli (from example shown in [E]).

(G) The disimilarity indices between mixture-evoked (blue bars) and single-odorant-evoked (gray bars) synchrony patterns for all animals (n = 8 moths) and units (n = 113, 750 unit pairs). Values are the means ± SEM. Asterisks denote a significant difference (Mann-Whitney U test: $p < 0.05$) between mixtures and single odorants.

pairs, however, did not significantly change the dissimilarity indices between the mixture and the control or between the mixture and the single odorant *ger* (representing 71% of the mixture headspace) (Kruskal-Wallis test: $p > 0.05$). Taken together, these results demonstrate that only relatively few cell pairs (<20) code for the mixture stimulus over the range of behaviorally relevant concentrations.

Conclusion

Odor concentrations in nature fluctuate over large distances, and it is generally accepted that in order to locate distant odor sources, the olfactory system in many animals must be able to maintain stimulus identity even with changing concentration. Neural mechanisms for intensity coding have been explored for single odorants in both insect and mammalian models, but it is not known how natural odor mixtures are represented in a consistent manner in the brain. Here, we demonstrate that the consistent behavioral response of a moth to a floral scent might be organized through a temporal coding mechanism that operates in moth AL networks. Whereas the majority of responses of single units to the mixtures was not different from responses to the single odorants and thus could not explain mixture-dependent behavior, population-level neural activity accurately discriminated among stimuli. Representation of a mixture through odor-evoked synchrony came in the form of a distinct temporal activity pattern that did not change over a behaviorally significant range of concentrations. In this manner, spatiotemporal representation provides a means for the olfactory system to bind disparate features of a complex stimulus into a coherent singular object.

Experimental Procedures

Electrophysiology—AL Ensemble Recording

The odor-evoked responses of 234 units were obtained in 16 male moths. In eight of the 16 moths the ensemble responses (n = 113 units) to synthetic monomolecular odorants and mixtures were examined. Recordings were made with 16-channel silicon multielectrode recording arrays (MRs) (Figure S10) (catalog number 4 × 4 - 3mm 50-177; NeuroNexus Technologies, Ann Arbor, MI) as previously described [18, 23].

Supplemental Data

Procedures for collection and analysis of floral headspace volatiles, procedures for electrophysiological experiments and analysis (experimental preparation, equipment, odor stimulation, and histological identification), and behavioral experiments are described in the Supplemental Experimental Procedures, available with this article online. Supplemental Data also include three tables and ten figures and are available with this article online at http://www.current-biology.com/supplemental/S0960-9822(09)00613-7.

Acknowledgments

We thank C. Reisenman, L. Abrell, R. Alarcón, J. Martin, and A. Dacks for their help in this project. V. Pawlowski and P. Jansma provided technical assistance. This work was supported by National Institutes of Health (NIH) grant DC-02751 (J.G.H.), National Science Foundation grant IOS 01-082270 (JAR), an NIH postdoctoral training grant (2 K12 GM000708-06), and a seed grant from the University of Arizona's Center for Insect Science.

Received: October 1, 2008
Revised: January 7, 2009
Accepted: January 8, 2009
Published online: February 19, 2009

References

1. Bartelt, R.J., Schaner, A.M., and Jackson, L.L. (1985). cis-Vaccenyl acetate as an aggregation pheromone in *Drosophila melanogaster*. J. Chem. Ecol. *11*, 1747–1756.
2. Boch, R., and Shearer, D.A. (1962). Identification of geraniol as the active component in the Nassanoff pheromone of the honey bee. Nature *194*, 704–706.
3. Kaissling, K.E. (1996). Peripheral mechanisms of pheromone reception in moths. Chem. Senses *21*, 257–268.
4. Laska, M., Fendt, M., Wieser, A., Endres, T., Hernandez Salazar, L.T., and Apfelbach, R. (2005). Detecting danger – or just another odorant? Olfactory sensitivity for the fox odor component 2,4,5-trimethylthiazoline in four species of mammals. Physiol. Behav. *84*, 211–215.
5. Williams, I.H., Pickett, J.A., and Martin, A.P. (1981). The Nasonov pheromone of the honey bee *Apis mellifera* L. (Hymenoptera, Apidae). Part II. Bioassay of the components using foragers. J. Chem. Ecol. *7*, 225–237.
6. Bathellier, B., Buhl, D.L., Accolla, R., and Carleton, A. (2008). Dynamic ensemble odor coding in the mammalian olfactory bulb: Sensory information at different timescales. Neuron *57*, 586–598.
7. Carlsson, M.A., and Hansson, B.S. (2003). Dose-response characteristics of glomerular activity in the moth antennal lobe. Chem. Senses *28*, 269–278.
8. Sachse, S., and Galizia, C.G. (2003). The coding of odour-intensity in the honeybee antennal lobe: local computation optimizes odour representation. Eur. J. Neurosci. *18*, 2119–2132.
9. Stopfer, M., Jayaraman, V., and Laurent, G. (2003). Intensity versus identity coding in an olfactory system. Neuron *39*, 991–1004.
10. Dasgupta, S., and Weddell, S. (2008). Learned odor discrimination in *Drosophila* without combinatorial odor maps in the antennal lobe. Curr. Biol. *18*, 1668–1674.
11. Raguso, R.A., Henzel, C., Buchman, S.L., and Nabhan, G.P. (2003). Trumpet flowers of the Sonoran Desert: Floral biology of *Peniocereus* Cacti and Sacred *Datura*. Int. J. Plant Sci. *164*, 877–892.
12. Riffell, J.A., Alarcon, R., Abrell, L., Davidowitz, G., Bronstein, J.L., and Hildebrand, J.G. (2008). Behavioral consequences of innate preferences and olfactory learning in hawkmoth-flower interactions. Proc. Natl. Acad. Sci. USA *105*, 3404–3409.
13. Lin, D.Y., Shea, S.D., and Katz, L.C. (2006). Representation of natural stimuli in the rodent main olfactory bulb. Neuron *50*, 937–949.
14. Lin, D.Y., Zhang, S.-Z., Block, E., and Katz, L.C. (2005). Encoding social signals in the mouse main olfactory bulb. Nature *434*, 470–477.
15. Mafra-Neto, A., and Cardé, R.T. (1994). Fine-scale structure of pheromone plumes modulates upwind orientation of flying moths. Nature *369*, 142–144.
16. Vickers, N.J., and Baker, T.C. (1994). Reiterative responses to single strands of odor promote sustained upwind flight and odor source location by moths. Proc. Natl. Acad. Sci. USA *91*, 5756–5760.
17. Duchamp-Viret, P., Duchamp, A., and Chaput, M.A. (2003). Single olfactory sensory neurons simultaneously integrate the components of an odour mixture. Eur. J. Neurosci. *18*, 2690–2696.
18. Lei, H., Christensen, T.A., and Hildebrand, J.G. (2004). Spatial and temporal organization of ensemble representations for different odor classes in the moth antennal lobe. J. Neurosci. *24*, 11108–11119.
19. Deisig, N., Giurfa, M., Lachnit, H., and Sandoz, J.C. (2006). Neural representation of olfactory mixtures in the honeybee antennal lobe. Eur. J. Neurosci. *24*, 1161–1174.
20. Cleland, T.A., Johnson, B.A., Leon, M., and Linster, C. (2007). Relational representation in the olfactory system. Proc. Natl. Acad. Sci. USA *104*, 1953–1958.
21. Christensen, T.A., Lei, H., and Hildebrand, J.G. (2003). Coordination of central odor representations through transient, non-oscillatory synchronization of glomerular output neurons. Proc. Natl. Acad. Sci. USA *100*, 11076–11081.
22. Friedrich, R.W., Habermann, C.J., and Laurent, G. (2004). Multiplexing using synchrony in the zebrafish olfactory bulb. Nat. Neurosci. *7*, 862–871.
23. Christensen, T.A., Pawlowski, V.M., Lei, H., and Hildebrand, J.G. (2000). Multi-unit recordings reveal context-dependent modulation of synchrony in odor-specific neural ensembles. Nat. Neurosci. *3*, 927–931.